Resolving the Fe XXV Triplet with Chandra in Cen X–3

R. Iaria[1], T. Di Salvo[1], N. R. Robba[1], L. Burderi[2], G. Lavagetto[1], A. Riggio[1]

ABSTRACT

We present the results of a 45 ks Chandra observation of the high-mass X-ray binary Cen X–3 at orbital phases between 0.13 and 0.40 (in the eclipse post-egress phases). Here we concentrate on the study of discrete features in the energy spectrum at energies between 6 and 7 keV, i.e. on the iron K_α line region, using the High Energy Transmission Grating Spectrometer on board the Chandra satellite. We clearly see a K_α neutral iron line at ~ 6.40 keV and were able to distinguish the three lines of the Fe XXV triplet at 6.61 keV, 6.67 keV, and 6.72 keV, with an equivalent width of 6 eV, 9 eV, and 5 eV, respectively. The equivalent width of the K_α neutral iron line is 13 eV, an order of magnitude lower than previous measures. We discuss the possibility that the small equivalent width is due to a decrease of the solid angle subtended by the reflector.

Subject headings: line: identification – line: formation – pulsars: individual (Centaurus X–3) — X-rays: binaries — X-rays: general

1. Introduction

Cen X–3 is an X-ray pulsar with an O-type supergiant companion. The orbital period is ~ 2.1 days and eclipses are observed. Out of eclipse, an iron emission line was detected at 6.5 ± 0.1 keV (Nagase et al., 1992; Burderi et al., 2000). Nagase et al. (1992) suggested that the feature at 6.5 keV, observed in the Ginga spectrum, could be fitted by two Gaussian lines centered at 6.4 keV and 6.67 keV, respectively, with the latter stronger than the former during the eclipse. The 6.5 keV line was found to be pulsating, supporting the fluorescence origin (Day et al., 1993) and implying that the fluorescence region does not uniformly surround the neutron star. Because of the large X-ray luminosity ($10^{37} - 10^{38}$ erg s^{-1}) and a strong

[1]Dipartimento di Scienze Fisiche ed Astronomiche, Università di Palermo, via Archirafi 36 - 90123 Palermo, Italy; email:iaria@fisica.unipa.it

[2]Università degli Studi di Cagliari, Dipartimento di Fisica, SP Monserrato-Sestu, KM 0.7, 09042 Monserrato, Italy

stellar wind from the companion, Day & Stevens (1993) proposed that photoionization of the circumstellar wind by X-ray irradiation will be significant in Cen X–3 system. Therefore, we expect the presence of emission lines due to recombination in highly ionized plasma. Ebisawa et al. (1996), using ASCA data taken at different orbital phases, identified the presence of three emission lines centered at around 6.40 keV (Fe I), 6.67 keV (Fe XXV), and 6.95 keV (Fe XXVI), respectively. The intrinsic width of each line was fixed at 0.01 keV, which was much smaller than the instrumental resolution. The equivalent widths (EWs) associated to the three lines were 105 eV, 78 eV, and 43 eV, respectively, at orbital phases between 0.14 and 0.18. Ebisawa et al. (1996) suggested that the line at 6.65 keV could be a blend of three lines at 6.63 keV, 6.67 keV, and 6.70 keV. The simultaneous presence of the Fe XXV and Fe XXVI lines in the spectrum implied a ionization parameter of the photoionized plasma of $\xi \sim 10^{3.4}$.

The common idea is that the K_α neutral iron line is produced in a low ionized region near the neutron star surface, because during the eclipse this line is weaker than out of the eclipse. On the other hand the Fe XXV and Fe XXVI lines are produced in a region far from the neutron star, probably in the photoionized wind of the companion star, because the intensities of these lines do not change with the orbital phase.

Recently Wojdowski et al. (2003), using Chandra data, analysed the spectrum of Cen X–3 during the eclipse. They resolved the Si XIII triplet and partially the Fe XXV triplet, concluding that the helium-like triplet component flux ratios outside of eclipse are consistent with emission from recombination and subsequent cascades (recombination radiation) from a photoionized plasma with a temperature of 100 eV. The best-fit velocity shifts and (Gaussian σ) velocity widths are generally less than 500 km s^{-1}. These velocities are significantly smaller than terminal velocities of isolated O star winds [$(1-2)\times 10^3$ km s^{-1}; e.g., Lamers et al. 1999].

In this work we present a spectral analysis of Cen X–3 in the 6–7 keV energy range from a 45 ks Chandra observation. The observation covers the orbital-phase interval 0.13–0.40. We detect the presence of the K_α neutral iron line at 6.4 keV and, for the first time, we resolve the triplet associated to the He-like ion of Fe XXV.

2. Observation

Cen X–3 was observed with the Chandra observatory on 2000 Dec 30 from 00:13:30 to 13:31:53 UT using the HETGS. The observation has a total integration time of 45.3 ks, and was performed in timed graded mode. The HETGS consists of two types of transmission

gratings, the Medium Energy Grating (MEG) and the High Energy Grating (HEG). The HETGS affords high-resolution spectroscopy from 1.2 to 31 Å (0.4–10 keV) with a peak spectral resolution of $\lambda/\Delta\lambda \sim 1000$ at 12 Å for HEG first order. The dispersed spectra were recorded with an array of six charge-coupled devices (CCDs) which are part of the Advanced CCD Imaging Spectrometer-S (Garmire et al., 2003)[1]. The current relative accuracy of the overall wavelength calibration is on the order of 0.05%, leading to a worst-case uncertainty of 0.004 Å in the 1st-order MEG and 0.006 Å in the 1st-order HEG. We processed the event list using available software (FTOOLS and CIAO v3.2 packages). We computed aspect-corrected exposure maps for each spectrum, allowing us to correct for effects from the effective area of the CCD spectrometer.

The brightness of the source required additional efforts to mitigate "photon pileup" effects. A 349 row "subarray" (with the first row = 1) was applied during the observation that reduced the CCD frame time to 1.3 s. The zeroth-order image is affected by heavy pileup: the event rate is so high that two or more events are detected in the CCD during the 1.3 s frame exposure. Pileup distorts the count spectrum because detected events overlap and their deposited charges are collected into single, apparently more energetic, events. Moreover, many events ($\sim 90\%$) are lost as the grades of the piled up events overlap those of highly energetic background particles and are thus rejected by the on board software. We therefore will ignore the zeroth-order events in the subsequent analysis. On the other hand, the grating spectra are not, or only moderately (less than 10 %), affected by pileup. In this work we utilize the HEG 1st-order spectrum in order to study the 6–7 keV energy range.

To determine the zero-point position in the image as precisely as possible, we calculated the mean crossing point of the zeroth-order readout trace and the tracks of the dispersed HEG and MEG arms. This results in the following source coordinates: R.A.= $11^h21^m15^s.095$, DEC=-60°37′25″.53 (J2000.0, with a 90% uncertainty circle of the absolute position of 0.6″[2]). Note that the Chandra position of Cen X–3 is distant ∼1.6″ from, and fully compatible with, the coordinates previously reported (Bradt & McClintock, 1983) based on the measure of the optical counterpart.

Finally we used the ephemeris of Nagase et al. (1992) to determine which orbital phase interval was covered by our observation. The observation covers the phases between 0.13 and 0.40; it was taken just after the egress from the eclipse, in the high, post-egress phase (see Nagase et al., 1992).

---

[1]See http://asc.harvard.edu/cdo/about_chandra for more details.

[2]See http://cxc.harvard.edu/cal/ASPECT/celmon/ for more details.

3. Spectral Analysis

We selected the 1st-order spectra from the HEG. Data were extracted from regions around the grating arms; to avoid overlapping between HEG and MEG data, we used a region size of 26 pixels for the HEG along the cross-dispersion direction. The background spectra were computed, as usual, by extracting data above and below the dispersed flux. The contribution from the background is 0.4% of the total count rate. We used the standard CIAO tools to create detector response files (Davis 2001) for the HEG -1 and HEG +1 order (background-subtracted) spectra. After verifying that these two spectra were compatible with each other in the whole energy range we coadded them using the script *add_grating_spectra* in the CIAO software; the resulting spectrum was rebinned to 0.0075 Å. Initially we fitted the 6–8 keV energy spectrum corresponding to the whole observation (orbital phases $\phi_{orb} = 0.13 - 0.40$) using a power-law component as a continuum. We fixed the equivalent hydrogen column to $N_H = 1.95 \times 10^{22}$ cm^{-2}, and the photon index to 1.2 as obtained by Burderi et al. (2000) from a BeppoSAX observation taken at similar orbital phases. The absorbed flux was $\sim 6.5 \times 10^{-9}$ ergs cm^{-2} s^{-1} in the 2–10 keV energy band, similar to 5.7×10^{-9} ergs cm^{-2} s^{-1} observed by Burderi et al. (2000) and one order of magnitude larger than that measured by ASCA at the orbital phase 0.14–0.18 ($\sim 8.4 \times 10^{-10}$ ergs cm^{-2} s^{-1}; see Ebisawa et al., 1996). In Fig. 1 (left panel) we show the spectrum and the residuals with respect to this model in the 6–7.6 keV energy range. It is evident the presence of a K_α neutral iron emission line at 6.4 keV with a width of 0.012 keV, and the presence of an absorption edge at 7.19 keV associated to low ionized iron (Fe II–Fe VI). We note that near 6.65 keV a more complex structure is present in the residuals; three peaks are evident. For this reason we used three Gaussian lines to fit these residuals. The energies of the lines are 6.61 keV, 6.67 keV, and 6.72 keV, the corresponding widths are < 0.018 keV, < 0.023 keV, and < 0.037 keV; finally, the corresponding EWs are 6 eV, 8.8 eV, and 4.8 eV. In Fig. 1 (right panel) we show the data and the residuals in the 6–7.6 keV energy range after adding the emission lines described above.

In Fig. 2 (left panel) we note the presence of a feature at 2 keV. We fitted this feature using two Gaussian lines centered at 2 keV and 2.006 keV (corresponding to Ly_{α_2} Si XIV and Ly_{α_1} Si XIV, respectively). The widths of these two lines are around 2 eV. In Table 1 we report the parameters of the emission lines and of the absorption edge.

The EW of the neutral iron K_α line is ~ 13 eV, that is a factor 8 and 14 lower than the EW of the neutral iron K_α line obtained during the ASCA (Ebisawa et al., 1996) and the Ginga observation (Nagase et al., 1992) taken in the egress and post-egress phases, respectively, and in which the unabsorbed flux of the continuum emission, in the 2–10 keV energy range, was $\sim 1 \times 10^{-9}$ and $\sim 4 \times 10^{-9}$ ergs cm^{-2} s^{-1}, respectively. It is a common idea

that the line at 6.4 keV is produced in the inner region of the system and that during dips and eclipses its flux decreases proportionally to the flux of the continuum, leaving unchanged the EW of the line at ~ 100 eV.

At the light of these results we have reanalyzed the previous Chandra observation (start time: 2000 Mar 5) of Cen X–3 during the pre-eclipse phases (between -0.16 and -0.12), already studied by Wojdowski et al. (2003) and corresponding to the "interval b" in their work (see Fig. 1 in Wojdowski et al., 2003). We fitted the 1st-order MEG and HEG data using a power-law component absorbed by an equivalent hydrogen column density fixed to 1.95×10^{22} cm^{-2} and by a partial covering component with an equivalent hydrogen column density of $(1.2 \pm 0.4) \times 10^{23}$ cm^{-2} and a covered fraction of the emitting region of 85 ± 6 %. The photon index of the power law was 0.43 and the unabsorbed flux in the 2–10 keV energy band was $\sim 1.8 \times 10^{-9}$ ergs cm^{-2} s^{-1}. As already discussed by Wojdowski et al. (2003), this spectrum shows a neutral iron K_α emission line at 6.384 ± 0.013 keV with a width of $\sigma < 39$ eV, a normalization of 9.4×10^{-4} ph cm^{-2} s^{-1}, and a EW of 42 ± 17 eV, respectively. As done by Ebisawa et al. (1996) for the spectrum during the pre-eclipse state, we also added the lines centered at 6.67 and 6.97 keV associated to Fe XXV and Fe XXVI, fixing the centroids at the expected values and the widths to 10 eV. We found upper limits on the line intensities of $\sim 4.2 \times 10^{-4}$ and $\sim 2.1 \times 10^{-4}$ ph cm^{-2} s^{-1}; moreover the inferred EWs are < 22 and < 11 eV, respectively for the Fe XXV and Fe XXVI emission lines. We conclude that these results are in absolute agreement with those reported by Ebisawa et al. (1996). However, the relatively low value (42 eV) of the EW of the neutral iron K_α emission line is indeed intermediate between the value measured by ASCA (75 eV) and the one we measure with Chandra (13 eV) and might indicate a trend of decreasing EW in 2000.

4. Discussion

We analyzed a 45 ks Chandra observation of the high mass X-ray binary Cen X–3. The position of the zeroth-order image of the source provides improved X-ray coordinates for Cen X–3 (R.A.= $11^h21^m15^s.095$, DEC=-60°37′25″.53), compatible with the optical coordinates previously reported for this source (see Bradt & McClintock, 1983). We performed a spectral analysis of the HEG 1st-order spectra of Cen X–3. The continuum emission was well fitted by a power-law component with a photon index of 1.2 absorbed by an equivalent hydrogen column density fixed at 1.95×10^{22} cm^{-2}. The inferred unabsorbed flux was $\sim 7.4 \times 10^{-9}$ ergs cm^{-2} s^{-1} in the 2–10 keV energy band, corresponding to a luminosity of 5.6×10^{37} ergs s^{-1} in the 2–10 keV energy band assuming a distance to the source of 8 kpc (Krzeminski, 1974). We detected a complex structure in the X-ray spectrum at 6–7.6 keV. In particular,

a K_α neutral iron emission line at 6.4 keV with a width of 12 eV, significantly different from zero and corresponding to a velocity dispersion of 1270 km s^{-1}. We also resolved the triplet of Fe XXV at about 6.6–6.7 keV. Furthermore we detected an absorption edge associated to Fe II–Fe VI.

We can explain the broad width of the K_α neutral iron line assuming that it was produced in an accretion disk. In fact, supposing that the width of the line was produced by a thermal velocity dispersion, then $T_4 \sim v^2/2.89$ K, where T_4 was the temperature in units of 10^4 K and v was the velocity dispersion in units of km s^{-1}. Since $v \sim 1270$ km s^{-1} for the K_α neutral iron line then the corresponding temperature should be $T \sim 5.6 \times 10^9$ K, physically not acceptable. On the other hand, assuming that the broadening is produced by the Keplerian motion of the accretion disk, we can infer the radius $r = GM/c^2(\Delta E/E)^{-2}$ where the line is produced; we find the inner radius of the reflecting region between 8.3×10^9 cm and 5.5×10^{10} cm, assuming for the source an inclination angle of 75^{+12}_{-13} degrees (see Nagase 1989). This radius is compatible with the upper limit of 3.4×10^{10} cm for the emission region of the K_α neutral iron line given by Nagase et al. (1992) and Day et al. (1993). Therefore, we conclude that the most probable origin of the 6.4 keV line is reflection from the outer accretion disk.

As noted in section 3 the low value of the EW of the 6.4 keV line measured in the Chandra observations of March and December 2000 might indicate that there is a trend of decreasing EW of the 6.4 keV line component in 2000. A possible explanation of the low EW observed during our observation might involve changes in the geometry of the reflector. Perhaps the solid angle subtended by the reflector with respect to the illuminating source changes with time (from 2π to less), maybe due to a precession of the accretion disk.

For the first time, thanks to the high energy resolution of Chandra, we were able to resolve the 6.6 keV line in the Cen X–3 spectrum as three lines centered at 6.61 keV, 6.67 keV, and 6.72 keV with an EW of 6 eV, 9 eV, and 5 eV. The Fe XXV He-like triplet is potentially a powerful diagnostic tool of density and temperature. We obtain that the intensities of the intercombination (i), resonance (r), and forbidden (f) lines are 7.6×10^{-4} photons cm^{-2} s^{-1}, 4.2×10^{-4} photons cm^{-2} s^{-1}, and 5.2×10^{-4} photons cm^{-2} s^{-1}, respectively. We find that $R \equiv f/i$ and $G \equiv (f + i)/r$ are 0.68 ± 0.39 and 3.05 ± 2.25 (where the uncertainties are at 90% confidence level for a single parameter). As Bautista & Kallman (2000) point out, caution should be exercised with the use of R and G as density and temperature diagnostics, respectively, since they are sensitive to whether the plasma is collisionally ionized or photoionized. Nevertheless the temperature curves in Bautista & Kallman (2000) indicate that T is between either 6.3×10^5 K and 1.5×10^7 K or 10^7 K and 4×10^7 K for collisional and photoionized gas, respectively. Because in the case of Cen X–3 (a bright X-ray source emitting near the Eddington limit) we are probably in the case of photoionized gas, we can conclude

that the temperature of the emitting region is $(1-4)\times10^7$ K. Furthermore the density curves are consistent with $n_e < 10^{17}$ cm^{-3}. Although we obtain a weak upper limit on the electron density this is compatible with the typical stellar wind density of $n_e = 10^{10} - 10^{11}$ cm^{-3}.

Finally we note that we do not observe the Fe XXVI line at 6.9 keV that was instead observed in the previous ASCA observation (Ebisawa et al., 1996). This implies that the stellar wind has, during our observation, a lower ionization parameter with respect to $\xi \sim 10^{3.4}$ estimated by Ebisawa et al. (1996). We estimate that ξ should be $\sim 10^{2.6} - 10^{2.8}$ (see fig. 7 in Ebisawa et al., 1996). This is also compatible with the detection of the Ly$_\alpha$ Si XIV at 2 keV. From $\xi = L_x/n_e^2 d$ (see Krolik et al., 1981), assuming a source luminosity of $L_x \sim 1.3\times10^{38}$ erg s^{-1} in the 0.1–200 keV energy band (see Burderi et al., 2000), a ionization parameter $\xi \simeq 10^{2.6} - 10^{2.8}$ and a separation between the neutron star, and the companion star of $d \simeq 10^{12}$ cm (Nagase et al., 1992), we find an electron density of the emitting region of 2×10^{11} cm^{-3}, in agreement with the previous results and compatible with the upper limit obtained above.

We thank the referee for the useful suggestions. This work was partially supported by the Italian Space Agency (ASI) and the Ministero della Istruzione, della Universitá e della Ricerca (MIUR).

REFERENCES

Bautista, M. A., & Kallman, T. R., 2000, ApJ, 544, 581

Bradt, H. V. D., & McClintock, J. E., 1983, ARA&A, 21, 13

Burderi, L., Di Salvo, T., Robba, N. R., et al., 2000, ApJ, 530, 429

Ebisawa, K., Day, C. S. R., Kallman, T. R., et al., 1996, PASJ, 48, 425

Day, C. S. R., & Stevens, I. R. 1993, ApJ, 403, 322

Day, C. S. R., Nagase, F., Asai, K., et al., 1993, ApJ, 408, 656

Davis, J. E. 2001, ApJ, 562, 575

Garmire, G. P., Bautz, M. W., Ford, et al., 2003, Proc. SPIE, 4851, 28

Krolik, J. H., McKee, C. F., & Tarter, C. B., 1981, ApJ, 249, 422

Krzeminski, W., 1974, ApJ, 192, L135

Lamers, H. J. G. L. M., Haser, S., de Koter, A., et al., 1999, ApJ, 516, 872

Nagase, F,. 1989, PASJ, 41, 1

Nagase, F., Corbet, R. H. D., Day, C. S. R., et al., 1992, ApJ, 396, 147

Wojdowski, P. S., Liedahl, D. A., Sako, M., et al., 2003, ApJ, 582, 959

Table 1. Results of the spectral fit.

Parameters	Phase Interval 0.13-0.40
Continuum	
$N_{\rm H}$ ($\times 10^{22}$ cm^{-2})	1.95 (fixed)
photon index	1.2 (fixed)
N_{po}	0.812 (fixed)
Fe II-Fe VI Absorption Edge	
E (keV)	$7.189^{+0.024}_{-0.041}$
τ	0.079 ± 0.018
K_α neutral iron line	
E (keV)	6.3975 ± 0.0033
σ (keV)	$0.0115^{+0.0045}_{-0.0042}$
I ($\times 10^{-3}$ cm^{-2} s^{-1})	$1.18^{+0.19}_{-0.17}$
EW (eV)	$13.2^{+2.1}_{-1.9}$
Fe XXV forbidden (f) line	
E (keV)	$6.6129^{+0.0072}_{-0.0041}$
σ (keV)	< 0.018
I ($\times 10^{-4}$ cm^{-2} s^{-1})	$5.2^{+2.1}_{-1.6}$
EW (eV)	$6.0^{+2.5}_{-1.8}$
Fe XXV intercomb. (i) line	
E (keV)	$6.6665^{+0.0067}_{-0.0036}$
σ (keV)	< 0.023
I ($\times 10^{-4}$ cm^{-2} s^{-1})	$7.6^{+2.2}_{-3.0}$
EW (eV)	$8.8^{+2.6}_{-3.5}$
Fe XXV resonance (r) line	
E (keV)	$6.720^{+0.010}_{-0.022}$
σ (keV)	< 0.037
I ($\times 10^{-4}$ cm^{-2} s^{-1})	$4.2^{+2.9}_{-1.8}$
EW (eV)	$4.8^{+3.3}_{-2.0}$
Si XIV Ly_{α_1} line	
E (keV)	$2.0008^{+0.0063}_{-0.0032}$
σ (keV)	$0.00175^{+0.00290}_{-0.00071}$
I ($\times 10^{-4}$ cm^{-2} s^{-1})	$2.3^{+1.0}_{-1.2}$
EW (eV)	$0.64^{+0.29}_{-0.32}$
Si XIV Ly_{α_2} line	
E (keV)	$2.0059^{+0.0400}_{-0.0021}$
σ (keV)	< 0.0019
I ($\times 10^{-4}$ cm^{-2} s^{-1})	$2.53^{+1.06}_{-0.81}$
EW (eV)	$0.71^{+0.29}_{-0.23}$

Note. — The model is composed of a power-law with absorption from neutral matter. Uncertainties are at 90% confidence level for a single parameter, upper limits are at 95% confidence level. N_{po} indicates the normalization of the power-law component in unit of photons keV^{-1} s^{-1} cm^{-2} at 1 keV. The parameters of the Gaussian emission lines are E, σ, I, and EW indicating the centroid in keV, the width in keV, the intensity of the line in units of photons s^{-1} cm^{-2}, and the EW in eV, respectively.

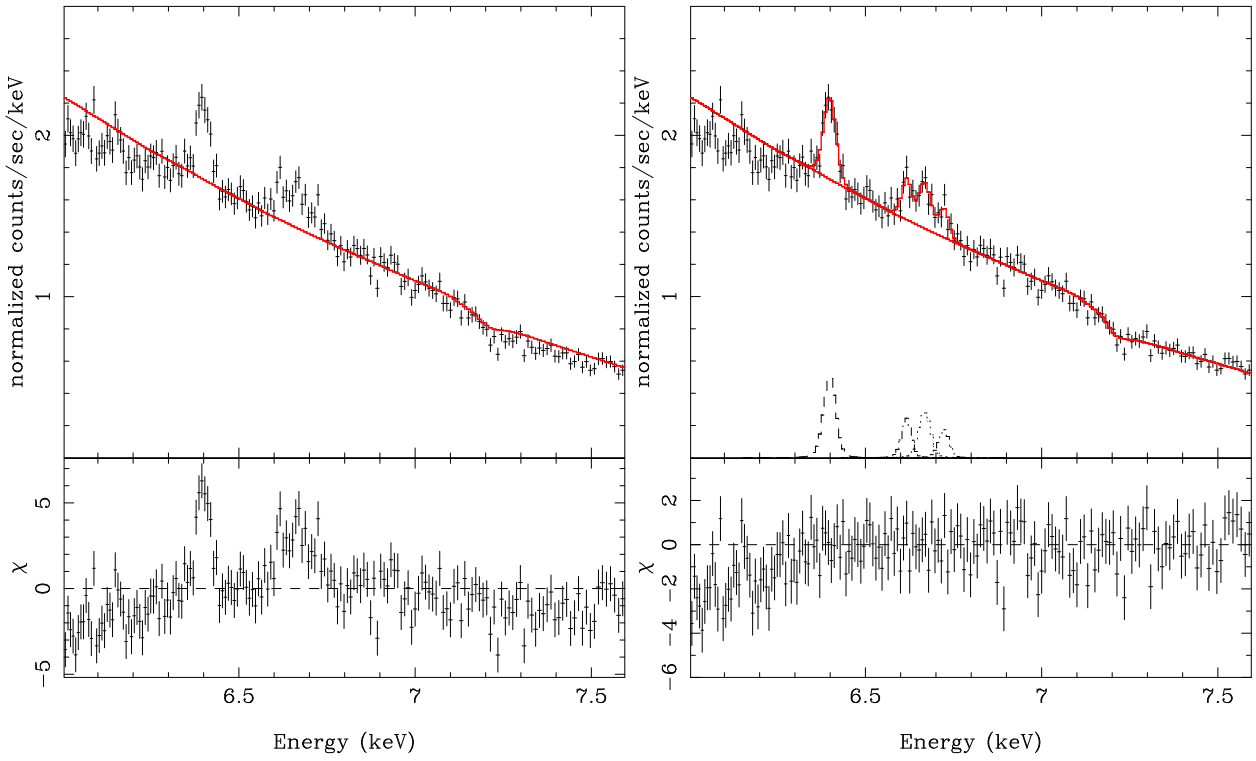

Fig. 1.— **Left Panel**: Data and residuals in the energy range 6.5–6.8 keV. The continuum emission is modelled by a power-law component. Two features are clearly evident at 6.4 keV, and 6.65 keV, respectively. **Right Panel**: The feature centered at 6.4 keV was modelled by a Gaussian line corresponding to the K_α neutral iron line. The broad feature centered at 6.65 keV can be modelled by three Gaussian lines at 6.61 keV, 6.67 keV, and 6.72 keV, respectively, corresponding to the Fe XXV triplet.

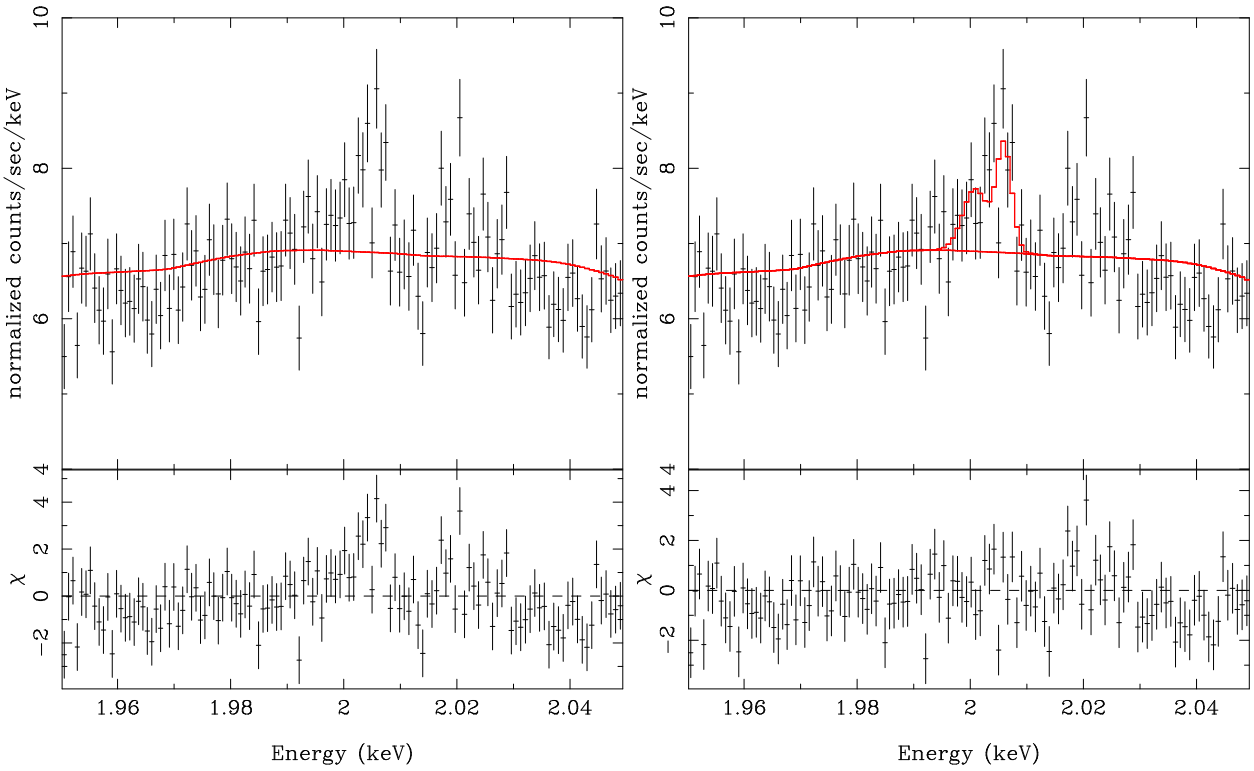

Fig. 2.— **Left Panel**: Data and residuals in the energy range 1.95–2.05 keV. A broad feature is present at 2 keV. **Right Panel**: The feature centered at 2 keV was modelled by two Gaussian lines corresponding to the Ly_{α_1} and Ly_{α_2} Si XIV.